Bioorganic & Medicinal Chemistry 21 (2013) 5725–5737

Contents lists available at ScienceDirect

Bioorganic & Medicinal Chemistry

journal homepage: www.elsevier.com/locate/bmc

Design, stereoselective synthesis, and biological evaluation of novel tri-cyclic compounds as inhibitor of apoptosis proteins (IAP) antagonists

Moriteru Asano [a,*], Kentaro Hashimoto [a], Bunnai Saito [a], Zenyu Shiokawa [a], Hiroyuki Sumi [a], Masato Yabuki [a], Mie Yoshimatsu [a], Kazunobu Aoyama [a], Teruki Hamada [a], Nao Morishita [a], Douglas R. Dougan [b], Clifford D. Mol [b], Sei Yoshida [a], Tomoyasu Ishikawa [a,*]

[a] Pharmaceutical Research Division, Takeda Pharmaceutical Company Limited, 26-1, Muraoka-higashi 2-chome, Fujisawa, Kanagawa 251-8555, Japan
[b] Structural Biology, Takeda California Inc., 10410 Science Center Drive, San Diego, CA 92121, USA

ARTICLE INFO

Article history:
Received 28 May 2013
Revised 9 July 2013
Accepted 10 July 2013
Available online 18 July 2013

Keywords:
Inhibitor of apoptosis proteins (IAP)
Octahydro-1*H*-cyclopropa[4,5]pyrrolo[1,2-*a*]pyrazine
Simmons–Smith cyclopropanation

ABSTRACT

We recently reported the discovery of octahydropyrrolo[1,2-*a*]pyrazine **A** as a lead compound for an inhibitor of apoptosis proteins (IAP) antagonist. To develop IAP antagonists with favorable PK profiles, we designed novel tri-cyclic compounds, octahydro-1*H*-cyclopropa[4,5]pyrrolo[1,2-*a*]pyrazines **1** and **2** based on co-crystal structural analysis of **A** with cellular IAP-1 (cIAP-1). The additional cyclopropane moiety was used to block the predicted metabolic site of compound **A** without detriment to the binding affinity for cIAP. Compounds **1** and **2** were stereoselectively synthesized via intermediates **4a** and **5b′**, which were obtained by Simmons–Smith cyclopropanation of ethylester **3a** and silyl ether **3b′**. Compounds **1** and **2** showed strong growth inhibition in MDA-MB-231 breast cancer cells and improved metabolic stability in comparison to **A**. Compound **2** exhibited significant in vivo PD effects to increase tumor necrosis factor-alpha mRNA in a dose dependent manner.

1. Introduction

Inhibitor of apoptosis proteins (IAPs) are anti-apoptotic regulators that block cell death.[1,2] Cellular IAP-1 (cIAP-1) and IAP-2 (cIAP-2) modulate tumor necrosis factor-alpha (TNFα) associated with the death receptor signaling pathway,[3,4] while the X-linked IAP (XIAP) suppresses apoptosis by binding to effectors caspase-3 and -7.[5,6] These proteins are up-regulated in various cancers and promote resistance to anti-cancer chemotherapy.[7] Therefore, IAP antagonists have potential utility as novel anticancer therapies.[8,9]

The second mitochondria-derived activator of caspases (Smac) is an endogenous inhibitor of IAPs.[10] It interacts with IAPs via its *N*-terminal Ala-Val-Pro-Ile (AVPI) tetrapeptide motif and antagonizes cIAP-1 and cIAP-2 by binding to the third baculoviral IAP repeats domain (BIR3) to induce rapid protein degradation.[11,12] Smac binds concurrently to both BIR2 and BIR3 of XIAP in a dimeric form, and inhibits contact of XIAP with caspase-3 and -7.[13] Recently, some small molecule mimics of the AVPI binding motif have been reported as antagonists of IAP protein.[14,15] Among these compounds, clinical evaluations of LCL-161 (Novartis),[16] GDC-0152 (Genentech),[17] HGS1029 (Aegera),[18] TL-32711 (Tetralogic)[19] and AT-406 (Ascenta/Michigan University)[20] are ongoing.

We began our search for potent novel IAP antagonists by analyzing the AVPI-XIAP co-crystal structure and designed a novel octahydropyrrolo[1,2-*a*]pyrazine scaffold as a surrogate for the 5-membered ring of proline in AVPI.[21,22] Our analysis suggested that the scaffold could enhance van der Waals contact with the IAP protein. After intensive optimization of this core scaffold, we successfully generated lead compound **A**, which showed strong binding inhibition of both XIAP and cIAP-1 and effectively induced cell death in the MDA-MB-231 human breast cancer cell line (Fig. 1).

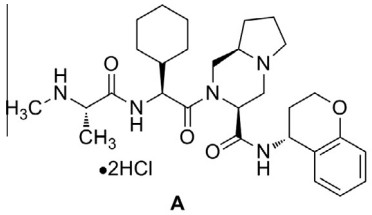

A

GI_{50} (cell growth, MDA-MB-231) = 5.7 nM
MS (human/mouse):128/116 μL/min/mg

Figure 1. Chemical structure and biological profiles of lead compound **A**.

* Corresponding authors. Tel.: +81 466 32 1152; fax: +81 466 294449 (M.A.); tel.: +81 466 32 1155; fax: +81 466 29 4449 (T.I.).
E-mail addresses: moriteru.asano@takeda.com (M. Asano), tomoyasu.ishikawa@takeda.com (T. Ishikawa).

0968-0896/$ - see front matter © 2013 Elsevier Ltd. All rights reserved.
http://dx.doi.org/10.1016/j.bmc.2013.07.020

However, this compound showed insufficient PK profiles due to its low metabolic stability. The octahydropyrrolo[1,2-*a*]pyrazine scaffold was predicted to be the main metabolic site for **A** based on liver microsome metabolite analysis.

Next, we analyzed the co-crystal structure of **A** with cIAP-1 (Fig. 2). To improve metabolic stability without reducing binding affinity, further modification of the octahydropyrrolo[1,2-*a*]pyrazine scaffold was justified because the analysis revealed it was exposed to the solvent area (Fig. 2B).

We designed unique tri-cyclic, octahydro-1*H*-cyclopropa[4,5]pyrrolo[1,2-*a*]pyrazine derivatives **1** and **2** (Fig. 3). The additional cyclopropane ring was expected to block the predicted metabolic site of octahydropyrrolo[1,2-*a*]pyrazine and improve its metabolic stability. In this report, we describe the stereoselective synthesis and biological profiles of compounds **1** and **2**.

2. Results and discussion

2.1. Chemistry

2.1.1. Synthetic scheme for octahydro-1*H*-cyclopropa[4,5]pyrrolo[1,2-*a*] pyrazine derivatives 1 and 2

The synthetic route to target compounds **1** and **2** is shown in Scheme 1. Our plan involves diastereoselective cyclopropanation of olefin **3**, which contains asymmetric functional groups at the *C*-2 position.[23] We expected stereoselective cyclopropanation would generate (1*R*,5*R*)-4 and (1*S*,5*S*)-5 in the key reaction and that stereoselectivity could be controlled by proper selection of the functional group of olefin **3**. From compounds **4** and **5**, diamines **4A** and **5A** could be prepared, followed by *N*-alkylation with methyl 2,3-dibromopropionate to yield the corresponding tri-cyclic derivatives **6** and **7**. Our targeted compounds **1** and **2** would be completed from compounds **6** and **7** by several formations of requisite amide side chains.

2.1.2. Investigation of stereoselective cyclopropanation

For the purpose of achieving stereoselecitive synthesis of (1*R*,5*R*)-**4** and (1*S*,5*S*)-**5**, we planned cyclopropanation of proline derived ethyl ester **3a** and silyl ether **3b′** with Simmons–Smith reagent (Scheme 2). Compounds **3a** and **3b′** were prepared from enantiomerically pure compounds **I** and **II** by the protocol previously reported.[24] Cyclopropanation of **3a** provided (1*R*,5*R*)-**4a** in 39% yield and its diastereomer (1*S*,5*S*)-**5a** in 7% yield after chromatographic separation. The selectivity was similar with the previous report.[25] These compounds **4a** and **5a** were smoothly transformed to the corresponding alcohols **4b** and **5b** by reduction with lithium aluminum hydride, respectively. On the other hand, cyclopropanation of **3b′** proceeded interestingly in reverse stereoselective manner, followed by deprotection of *tert*-butyldimethylsilyl (TBS) group with tetra-*n*-butylammonium fluoride (TBAF) to afford desired alcohol (1*S*,5*S*)-**5b** along with the corresponding diastereomer (1*R*,5*R*)-**4b** as a minor product (two steps 68% yield from **3b′**, **4b**/**5b** = 1:5). Although these compounds (1*S*,5*S*)-**5b** and (1*R*,5*R*)-**4b** were inseparable in this step, the ratio of compounds **5b**/**4b** was determined by ^{1}H NMR data.

As shown in Scheme 3, cyclopropanations of **3a** and **3b′** are supposed to proceed through transition state **3aTS** and **3b′TS**, respectively and generate (1*R*,5*R*)-**4a** and (1*S*,5*S*)-**5b′** stereoselectively. In the case of cyclopropantion of **3a**, zinc of Simmons–Smith reagent might co-ordinate with the carbonyl oxygen of ethyl ester group and would be more accessible to the β-face than the α-face of compound **3a**.[26] On the other hand, we can explain that α-face selective cyclopropanation of **3b′** should be preferred since the silyl ether group of **3b′** stands almost perpendicular to the five membered ring and blocks an approach of Simmons–Smith reagent from β-face.

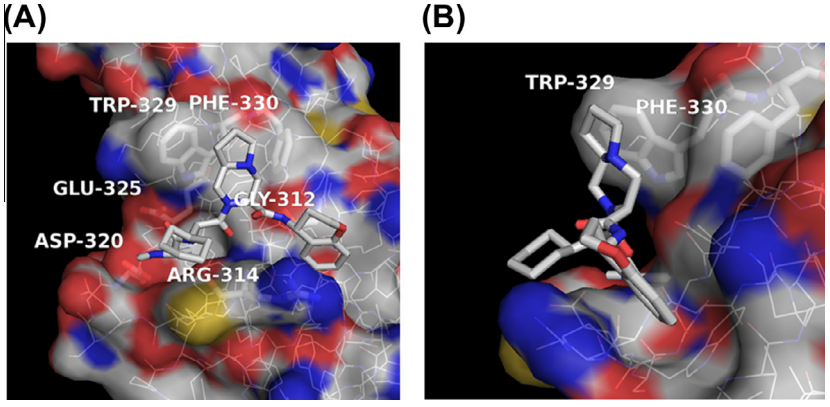

Figure 2. Co-crystal structure of compound **A** with cIAP-1 (PDB code 4LGU, 2.00 Å resolution): (A) compound **A** binds efficiently to cIAP-1. (B) The octahydropyrrolo[1,2-*a*]pyrazine scaffold is exposed to solvent area.

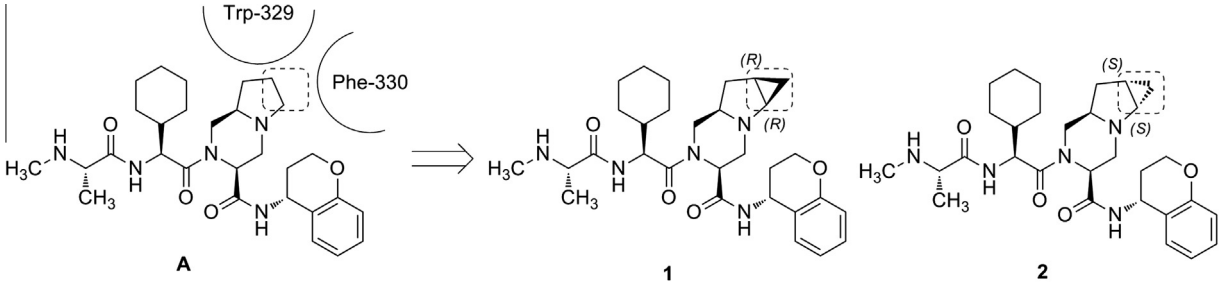

Figure 3. Design of octahydro-1*H*-cyclopropa[4,5]pyrrolo[1,2-*a*]pyrazine derivatives **1** and **2**.

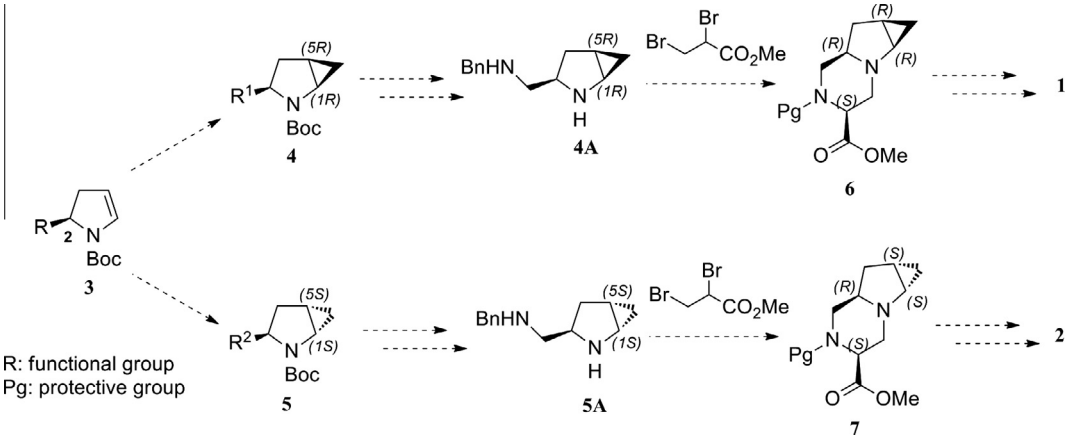

Scheme 1. Synthetic plan for tri-cyclic compounds **1** and **2**.

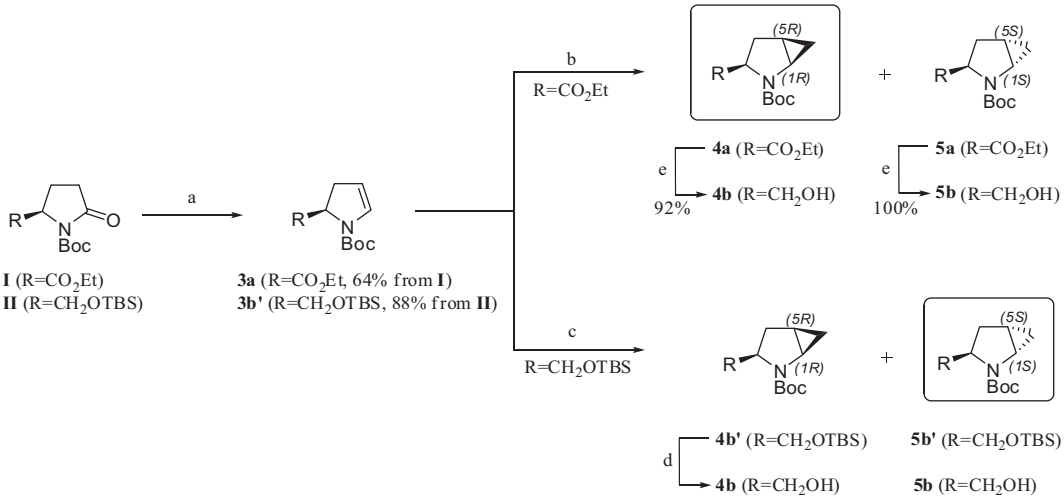

Scheme 2. Stereoselective synthesis of (1*R*,5*R*)-**4b** and (1*S*,5*S*)-**5b** Reagents and conditions: (a) $LiEt_3BH$, THF, −78 °C then DIPEA, DMAP, TFAA, room temperature; (b) Et_2Zn, CH_2I_2, toluene, 0 °C–room temperature, 4 h, 39% (**4a**), 7% (**5a**) (**4a**/**5a** = 5:1); (c) Et_2Zn, CH_2I_2, toluene, 0 °C → room temperature, 3 h; (d) TBAF, THF, room temperature, 30 min, 2 steps 68% from **3b′** (**4b**/**5b** = 1:5); (e) $LiAlH_4$, THF, 0 °C, 30 min.

2.1.3. Construction of tri-cyclic octahydro-1*H*-cyclopropa[4,5]pyrrolo[1,2-*a*] pyrazine scaffold

With cyclopropanes **4b** and **5b** in hand, we next directed our attention to construction of tri-cyclic octahydro-1*H*-cyclopropa[4,5]pyrrolo[1,2-*a*]pyrazine scaffold (Scheme 4). To prepare the precursor diamine, alcohols **4b** and **5b** were converted to the corresponding aldehydes by oxidation with sulfur trioxide pyridine complex (SO_3·Py) which were followed by reductive amination with benzylamine to generate (1*R*,5*R*)-**4c** and (1*S*,5*S*)-**5c** in 85% and 58% yields in 2 steps, respectively. Construction of octahydro-1*H*-cyclopropa[4,5]pyrrolo[1,2-*a*]pyrazine scaffold was carried out by *N*-Boc deprotection and the subsequent alkylation with methyl 2,3-dibromopropioate under basic conditions at 90 °C. The reactions proceeded regioselectively and provided the desired compounds (1*aR*,7*aR*)-**8a** and (1*aS*,7*aS*)-**9a** along with a considerable amount of their respective diastereomers **8b** and **9b**. The *C*-4 stereochemistry of **8** and **9** was confirmed by NOE experiments, where the axial hydrogen at the *C*-4 positon of **8b** and **9b** showed NOE correlations with the *C*-6 axial hydrogen, while the *C*-4 equatorial hydrogen of **8a** and **9a** displayed no NOE interaction with axial hydrogen atom at the *C*-6 position.[27] The obtained compounds **8a** and **9a** were readily converted to the key intermediates **6** and **7** by hydrogenative removal of the benzyl group and the subsequent Boc protection of the produced amines in 85% and 86% yield, respectively. Similar transformation of diastereomers **8b** and **9b** provided compounds **8c** and **9c** which were treated with sodium methoxide to give additional amount of the desired compound **6** and **7** in 26% and 62% yield by epimerization at *C*-4 position, respectively.

To better understand the reason why the compounds **8c** and **9c** can be converted to compounds **6** and **7** effectively, we calculated minimum energy of octahydro-1*H*-cyclopropa[4,5]pyrrolo[1,2-*a*]pyrazine derivatives as shown in Figure 4A and B. Compounds **6** and **7** were thermodynamically more stable than compounds **8c** and **9c** with around 4 kcal/mol energy. We considered that methyl ester groups of **6** and **7** can be placed in axial position without steric hindrance by *N*-*tert* butoxy group (confromations shown on righthand side), while those of **8c** and **9c** were placed in equatorial one to cause a steric repulsion (conformations shown on left-hand side).

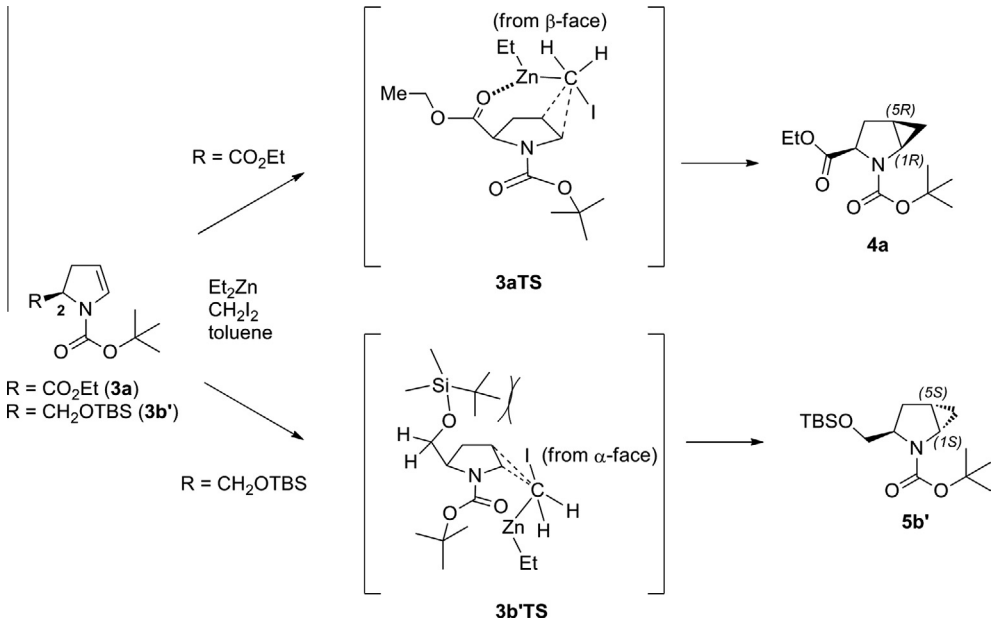

Scheme 3. Proposed reaction mechanism on cyclopropanation of **3a** and **3b′**.

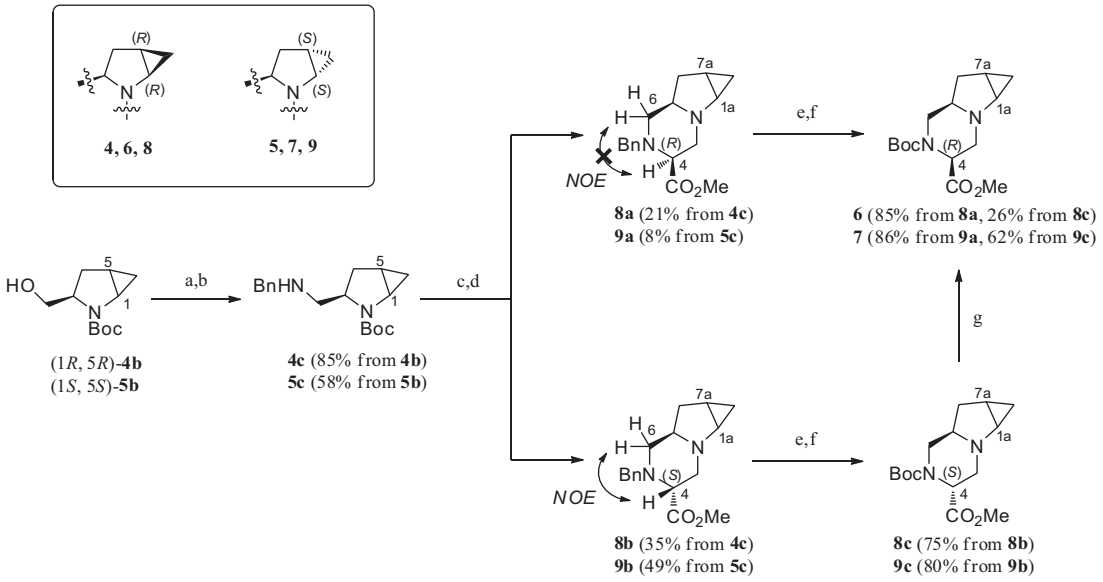

Scheme 4. Synthesis of key intermediates **6** and **7**. Reagents and conditions: (a) SO_3·Py, Et_3N, DMSO-EtOAc, 0 °C–room temperature; (b) $NaBH(OAc)_3$, benzylamine, THF, room temperature; (c) HCl–EtOAc, room temperature; (d) methyl 2,3-dibromopropioate, Et_3N, toluene, 90 °C; (e) H_2, 10% Pd/C, 5% HCl–MeOH, room temperature; (f) Boc_2O, $NaHCO_3$, THF-H_2O, room temperature; (g) NaOMe, MeOH, 60 °C.

2.1.4. Conversion to target compounds 1 and 2

The obtained key intermediates **6** and **7** were converted into the target octahydro-1*H*-cyclopropa[4,5]pyrrolo[1,2-*a*]pyrazine derivatives **1** and **2** as described in Scheme 5. Hydrolysis of methyl esters **6** and **7** with aqueous lithium hydroxide was followed by their amide condensation with (*R*)-chroman-4-amine hydrochloride (**10**) to afford compounds **11** and **12** in 18% and 94% yield from compounds **6** and **7**, respectively. The absolute configuration of **12** was confirmed by X-ray crystallographic analysis. Subsequent *N*-Boc deprotection and repetitive amide formations of **11** and **12** with Boc-protected cyclohexyl glycine **13** and *N*-methyl alanine **16** provided the desired compounds **17** and **18** in 4 steps. Finally, synthesis of the target compounds **1** and **2** as dihydrochloride salt was achieved by *N*-Boc deprotection of **17** and **18** with 4 M HCl in EtOAc in 76% and 65% yield, respectively.

2.2. Biological activity

2.2.1. In vitro assay

The biological in vitro activity of compounds **1** and **2** was evaluated. In time-resolved fluorescence resonance energy transfer (HTRF) assay, binding inhibition of XIAP and cIAP-1 was measured by detecting competitive displacement of biotinyl-Smac from human XIAP_BIR3 or cIAP-1_BIR3 domain protein, and data were reported as the IC_{50} value. MDA-MB-231 human breast cancer cells

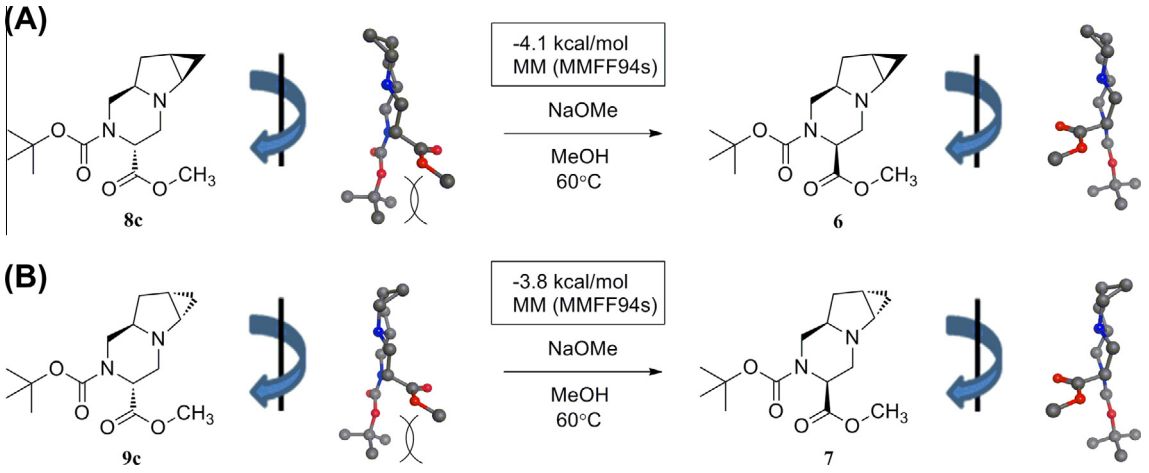

Figure 4. Analysis of epimerization based on calculations of minimum energy: (A) **8c** → **6**, (B) **9c** → **7**.

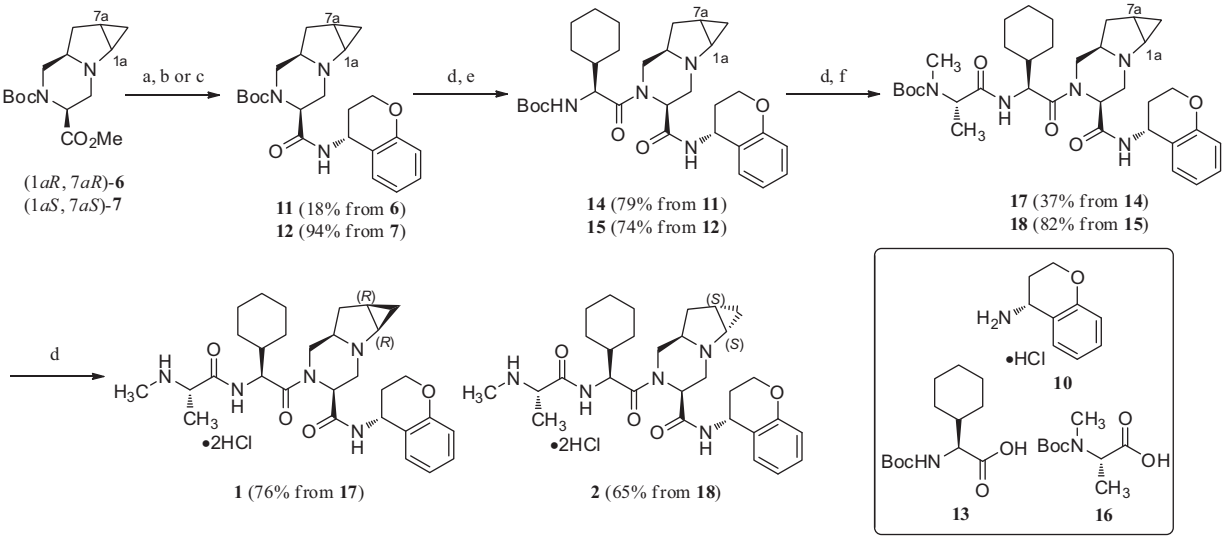

Scheme 5. Synthesis of target compounds **1** and **2**. Reagents and conditions (a) LiOH·H_2O, THF-H_2O, 50 °C, 5 h; (b) (*R*)-chroman-4-amine hydrochloride (**10**), WSC, 1-hydroxybenzotriazole, DIPEA, DMF, room temperature, 18 h; (c) (*R*)-chroman-4-amine hydrochloride (**10**), HATU, DIPEA, DMF, room temperature, 18 h (d) HCl–EtOAc, room temperature; (e) Boc-D-cyclohexyl glycine (**13**), HATU, DIPEA, DMF, room temperature; (f) Boc-L-methyl alanine (**16**), HATU, DIPEA, DMF, room temperature.

were used in cell growth assays, and activities were expressed as the GI_{50} values. These data are summarized along with metabolic stability data in Table 1.

As expected, tri-cyclic octahydro-1*H*-cyclopropa[4,5]pyrrolo[1,2-*a*]pyrazine derivatives **1** and **2** exhibited improved metabolic stability in comparison to lead compound **A**. Moreover, compound **2** maintained comparable potency in IAP binding and cell growth assays.

The binding conformation of **2** with cIAP-1 is depicted as an X-ray protein–ligand complex co-crystal structure with cIAP-1 in Fig. 5. The co-crystal structure indicated that the binding mode of compound **2** was almost similar to that of lead compound **A** and the additional cyclopropane moiety was located in the solvent area without conflicting with cIAP-1 as we expected.

2.2.2. In vivo PD study: inducement of TNFα with compound 2

To investigate the in vivo PD profiles of octahydro-1*H*-cyclopropa[4,5]pyrrolo[1,2-*a*]pyrazine derivative **2**, mRNA induction of TNFα with **2** was measured with an MDA-MB-231-Luc human breast cancer cell xenograft model in mice (Fig. 6). Oral administration of compound **2** showed a significant dose-dependent increase in TNFα mRNA in comparison to the vehicle control.

3. Conclusion

We designed novel tri-cyclic octahydro-1*H*-cyclopropa[4,5]pyrrolo[1,2*a*]pyrazine derivatives **1** and **2** as IAP antagonist and developed their enantioselective synthesis. Both compounds exhibited improved metabolic stability in comparison to the lead octahydropyrrolo[1,2-*a*]pyrazine compound **A**. Furthermore, compound **2** maintained IAP binding inhibition and cellular potency comparable to that of compound **A**. In addition, co-crystals of compound **2** with cIAP-1 could explain the stronger binding inhibition of **2** in comparison to the corresponding diastereomer **1**. Reflecting its in vitro potency, compound **2** was proven effective in vivo, where it induced significant TNFα transcription in an MDA-MB-231-Luc human breast cancer cell xenograft model in mice. Further modification of tri-cyclic compound **2** may yield an effective novel IAP antagonist treatment.

Table 1
Biological properties of tri-cyclic compounds **1** and **2**[a]

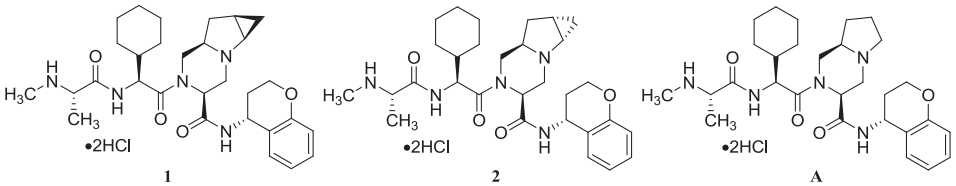

Compound	Binding (HTRF) IC_{50} (nM)		Cell growth inhibition GI_{50} (nM)	Metabolic stability (μL/min/mg)	
	XIAP	cIAP-1	MDA-MB-231	Human	Mouse
1	650 (510–840)	28 (21–38)	83 (66–110)	39	45
2	350 (280–440)	3.5 (3.2–3.7)	7.8 (3.6–17)	72	96
A	240 (190–300)	2.1 (1.8–2.4)	5.7 (4.9–6.7)	128	116

[a] Numbers in parentheses represent 95% confidence interval.

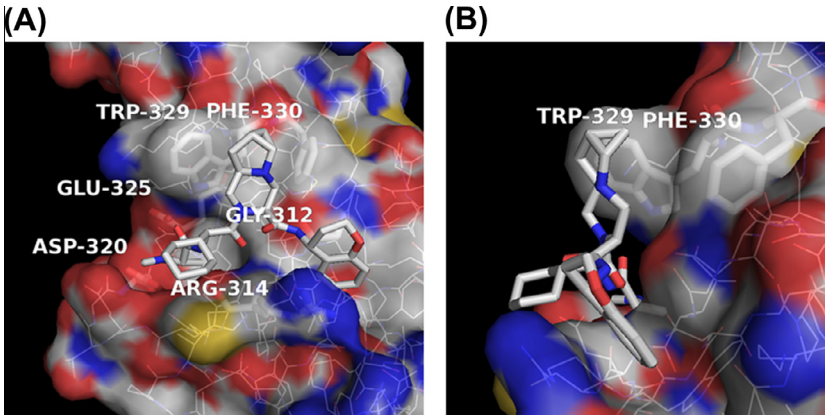

Figure 5. Co-crystal structure of tri-cyclic compound **2** with cIAP-1 (PDB code 4LGE, 1.55 Å resolution): (A) The binding mode is almost similar to that of lead compound **A**. (B) The cyclopropane moiety is located in the solvent area without conflicting with cIAP-1.

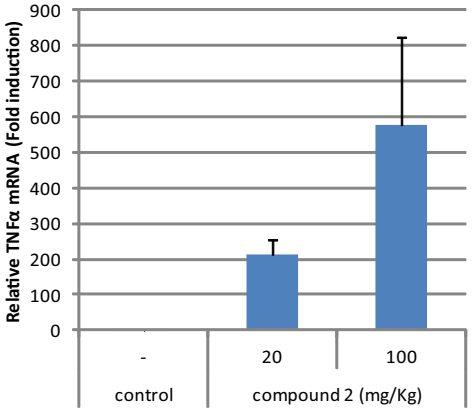

Figure 6. Compound **2** showed significant increase of TNF-α mRNA in a dose dependent manner. Dose level 20 mg/kg, $P \leqslant 0.025$ versus control; 100 mg/kg, $P \leqslant 0.005$ versus control (Shirley–Williams test).

4. Experimental

^{1}H nuclear magnetic resonance (NMR) spectra was measured on a Bruker DPX-300 or a Bruker AV-600 spectrometer; chemical shifts are given in ppm with tetramethylsilane as an internal standard, and coupling constants (*J*) are measured in hertz (Hz). The following abbreviations are used: s = singlet, d = doublet, t = triplet, q = quartet, m = multiplet and br s = broad singlet. ^{13}C NMR was measured on a Bruker AV-600 spectrometer; chemical shifts are given in ppm with $CDCl_3$ as an internal standard. High-resolution mass spectrometry analyses were carried out by Takeda Analytical Research Laboratories, Ltd. Reaction progress was determined by thin layer chromatography (TLC) analysis on silica gel 60 F_{254} plate (Merck Ltd) or NH TLC plates (Fuji Silysia chemical Ltd). Chromatographic purification was carried on silica gel columns 60 (0.063–0.200 mm or 0.040–0.063 mm, Merck Ltd), basic silica gel (ChromatorexNH, 100–200 mesh, Fuji silysia chemical Ltd) or Purif-Pack (SI 60 μM or NH 60 μM, Fuji Silysia chemical Ltd). Mass spectra (MS) were acquired using an Agilent LC/MS system (Agilent1200SL/Agilent6130MS), Shimadzu LC/MS system (LC-10ADvp high pressure gradient system/LCMS-2010A) or Shimadzu UFLC/MS (Prominence UFLC high pressure gradient system/LCMS-2020) operating in electron spray ionization mode (ESI+) and were used to confirm the purity of each compound. The column used was an L-column 2 ODS (3.0 × 50 mm I.D, 3 μm, CERI, Japan) with a temperature of 40 °C and a flow rate of 1.2 or 1.5 mL/min. Mobile phase A was 0.05% TFA in ultrapure water. Mobile phase B was 0.05% TFA in acetonitrile which was increased linearly from 5% to 90% over 2 min, 90% over the next 1.5 min, after which the column was equilibrated to 5% for 0.5 min. Commercial reagents and solvents were used without additional purification. Abbreviations are used as follows: HATU, *O*-(7-azabenzotriazol-1-yl)-*N*,*N*,*N*′,*N*′-tetramethyluronium hexafluorophosphate; WSC, 1-(3-dimethylaminopropyl)-3-ethylcarbodimide hydrochloride; DMAP,

4-(*N*,*N*-dimethylamino)pyridine; DIPEA, *N*-ethyldiisopropylamine; TFAA, trifluoroacetic anhydride.

4.1. (1*aR*,4*S*,6*aR*,7*aR*)-5-{(2*S*)-2-Cyclohexyl-2-[(*N*-methyl-L-alanyl)amino]acetyl}-*N*-[(4*R*)-3,4-dihydro-2*H*-chromen-4-yl]octahydro-1*H*-cyclopropa[4,5]pyrrolo[1,2-*a*]pyrazine-4-carboxamide dihydrochloride (1)

To a solution of *tert*-butyl[(1*S*)-2-{[(1*S*)-1-cyclohexyl-2-{(1*aR*,4*S*,6*aR*,7*aR*)-4-[(4*R*)-3,4-dihydro-2*H*-chromen-4-ylcarbamoyl]octahydro-5*H*-cyclopropa[4,5]pyrrolo[1,2-*a*]pyrazin-5-yl}-2-oxoethyl]amino}-1-methyl-2-oxoethyl]methylcarbamate (**17**, 77.1 mg, 0.121 mmol) in EtOAc (5.0 mL) was added 4 M HCl in EtOAc (10 mL, 40 mmol), and the reaction mixture was stirred at room temperature for 1.5 h. The mixture was concentrated in vacuo, and the precipitated solid was collected by filtration, washed with Et_2O and dried under vacuum to give **1** (56.4 mg, 76%) as pale yellow amorphous solid.

^{1}H NMR (300 MHz, DMSO-d_6) δ 0.78–1.44 (14H, m), 1.48–2.12 (12H, m), 3.05–4.40 (7H, m), 4.45–4.65 (1H, m), 4.64–4.83 (1H, m), 4.87–5.09 (1H, m), 6.69–6.98 (2H, m), 7.03–7.27 (2H, m), 8.62–8.94 (3H, m), 8.98–9.31 (1H, m), 12.60–12.84 (1H, m); HRMS-ESI (*m*/*z*): [M+H] calcd for $C_{30}H_{43}N_5O_4$, 538.3388, found 538.3384.

4.2. (1*aS*,4*S*,6*aR*,7*aS*)-5-{(2*S*)-2-Cyclohexyl-2-[(*N*-methyl-L-alanyl)amino]acetyl}-*N*-[(4*R*)-3,4-dihydro-2*H*-chromen-4-yl]octahydro-1*H*-cyclopropa[4,5]pyrrolo[1,2-*a*]pyrazine-4-carboxamide dihydrochloride (2)

To a solution of *tert*-butyl[(1*S*)-2-{[(1*S*)-1-cyclohexyl-2-{(1*aS*,4*S*,6*aR*,7*aS*)-4-[(4*R*)-3,4-dihydro-2*H*-chromen-4-ylcarbamoyl]octahydro-5*H*-cyclopropa[4,5]pyrrolo[1,2-*a*]pyrazin-5-yl}-2-oxoethyl]amino}-1-methyl-2-oxoethyl]methylcarbamate (**18**, 220 mg, 0.345 mmol) in EtOAc (10 mL) was added 4 M HCl in EtOAc (20 mL, 80 mmol), and the reaction mixture was stirred at room temperature for 3 h. The mixture was concentrated in vacuo, and the precipitated solid was collected by filtration, washed with *i*-Pr_2O and dried under vacuum to give **2** (173 mg, 65%) as colorless amorphous solid.

^{1}H NMR (300 MHz, DMSO-d_6) δ 0.76–2.57 (26H, m), 2.94–4.30 (6H, m), 4.37–4.60 (1H, m), 4.63–4.96 (2H, m), 4.91–5.09 (1H, m), 6.47–7.02 (2H, m), 7.05–7.65 (2H, m), 8.40–8.96 (3H, m), 9.04–9.37 (1H, m), 11.64–12.60 (1H, m); HRMS-ESI (*m*/*z*): [M+H] calcd for $C_{30}H_{43}N_5O_4$, 538.3388, found 538.3388.

4.3. 1-*tert*-Butyl 2-ethyl(2*R*)-2,3-dihydro-1*H*-pyrrole-1,2-dicarboxylate (3a)

To a solution of 1-*tert*-butyl 2-ethyl (2*R*)-5-oxopyrrolidine-1,2-dicarboxylate **I** (21.3 g, 82.6 mmol) in toluene (165 mL) was added dropwise 1.0 M lithium triethylborohydride in THF (90.9 mL, 90.9 mmol) at −78 °C, and the reaction mixture was stirred at the same temperature for 1 h. After addition of DMAP (201 mg, 1.65 mmol) and DIPEA (64.1 g, 496 mmol) successively, TFAA (13.7 mL, 98.4 mmol) was added slowly to the solution. The resulting mixture was stirred at room temperature for 3 h. The mixture was partitioned between water (300 mL) and EtOAc (300 mL), and the organic layer was dried over $MgSO_4$, and concentrated in vacuo. The residue was purified by column chromatography (*n*-Hexane/EtOAc = 100:0 → 34:66) to give **3a** (13.8 g, 69%) as pale yellow oil.

^{1}H NMR (300 MHz, $CDCl_3$) δ 1.19–1.35 (3H, m), 1.40–1.54 (9H, m), 2.53–2.75 (1H, m), 2.95–3.18 (1H, m), 4.10–4.33 (2H, m), 4.50–4.70 (1H, m), 4.85–4.99 (1H, m), 6.46–6.71 (1H, m).

4.4. *tert*-Butyl(2*R*)-2-({[*tert*-butyl(dimethyl)silyl]oxy}methyl)-2,3-dihydro-1*H*-pyrrole-1-carboxylate (3b′)

To a solution of *tert*-butyl(2*R*)-2-({[*tert*-butyl(dimethyl)silyl]oxy}methyl)-5-oxopyrrolidine-1-carboxylate **II** (1.01 g, 3.07 mmol) in toluene (20 mL) was added dropwise 1.0 M lithium triethylborohydride in THF (3.37 mL, 3.37 mmol) at −70 °C, and the reaction mixture was stirred at the same temperature for 1 h. After addition of DMAP (10.0 mg, 0.082 mmol) and DIPEA (2.38 g, 18.4 mmol) successively, TFAA (0.508 mL, 3.68 mmol) was added slowly to the mixture. The resulting mixture was stirred at room temperature for 1 h. The mixture was partitioned between water (30 mL) and EtOAc (30 mL), and the organic layer was dried over $MgSO_4$, and concentrated in vacuo. The residue was purified by column chromatography (*n*-Hexane/EtOAc = 100:0 → 50:50) to give **3b′** (0.85 g, 88%) as colorless oil.

^{1}H NMR (300 MHz, $CDCl_3$) δ 0.04 (3H, s), 0.05 (3H, s), 0.87 (9H, s), 1.48 (9H, s), 2.51–2.84 (2H, m), 3.43–3.57 (1H, m), 3.66–3.79 (1H, m), 4.03–4.27 (1H, m), 4.83–4.99 (1H, m), 6.33–6.58 (1H, m).

4.5. 2-*tert*-Butyl 3-ethyl(1*R*,3*R*,5*R*)-2-azabicyclo[3.1.0]hexane-2,3-dicarboxylate (4a) and 2-*tert*-butyl 3-ethyl(1*S*,3*R*,5*S*)-2-azabicyclo[3.1.0]hexane-2,3-dicarboxylate (5a)

To a solution of **3a** (13.8 g, 57.2 mmol) in toluene (400 mL) was added dropwise 1.1 M diethylzinc solution in toluene (114 mL, 126 mmol) at −40 °C, and the reaction mixture was stirred at the same temperature for 30 min. After addition of diiodomethane (61.3 g, 229 mmol) in toluene (50 mL) at −40 °C, the reaction mixture was stirred at −40 °C–−20 °C for 30 min, at 0 °C for 2 h and at room temperature for 2 h. To the reaction mixture was added satd $NaHCO_3$ (500 mL) and EtOAc (500 mL), and the mixture was filtered through a pad of Celite®. The filtrate was separated, and the organic layer was dried over $MgSO_4$, and concentrated in vacuo. The residue was purified by column chromatography (*n*-Hexane/EtOAc = 98:2 → 50:50) to give **4a** (5.69 g, 39%, colorless oil) and **5a** (1.09 g, 7%, colorless oil).

4a: ^{1}H NMR (300 MHz, $CDCl_3$) δ 0.62–0.79 (1H, m), 0.85–0.94 (1H, m), 1.22–1.31 (3H, m), 1.39–1.56 (10H, m), 1.98–2.06 (1H, m), 2.48–2.68 (1H, m), 3.41–3.59 (1H, m), 4.09–4.25 (2H, m), 4.45–4.66 (1H, m).

5a: ^{1}H NMR (300 MHz, $CDCl_3$) δ 0.39–0.53 (1H, m), 0.72–0.88 (1H, m), 1.19–1.33 (3H, m), 1.37–1.65 (10H, m), 2.14–2.29 (1H, m), 2.28–2.42 (1H, m), 3.37–3.59 (1H, m), 3.91–4.12 (1H, m), 4.08–4.28 (2H, m).

4.6. *tert*-Butyl(1*R*,3*R*,5*R*)-3-(hydroxymethyl)-2-azabicyclo[3.1.0]hexane-2-carboxylate (4b)

To an ice-cooling mixture of lithium aluminum hydride (1.68 g, 44.26 mmol) in THF (120 mL) was added dropwise a solution of **4a** (5.55 g, 21.74 mmol) in THF (20 mL), and the reaction mixture was stirred at 0 °C for 30 min. After addition of sodium carbonate decahydrate (25 g), the mixture was stirred for 1 h and filtrated through a pad of Celite® with THF. The filtrate was concentrated in vacuo, and the residue was purified by column chromatography (*n*-Hexane/EtOAc = 98:2 → 34:66) to give **4b** (4.26 g, 92%) as colorless oil.

^{1}H NMR (300 MHz, $CDCl_3$) δ 0.40 (1H, br s), 0.73–0.85 (1H, m), 1.38–1.70 (3H, m), 1.50 (9H, s), 2.38–2.51 (1H, m), 3.39–3.54 (2H, m), 4.28–4.41 (1H, m), 4.77–4.89 (1H, m).

4.7. *tert*-Butyl(1*S*,3*R*,5*S*)-3-(hydroxymethyl)-2-azabicyclo[3.1.0]hexane-2-carboxylate (5b)

(Method A: **5a** → **5b**)

To a mixture of lithium aluminum hydride (298 mg, 7.85 mmol) in THF (20 mL) was added dropwise a solution of **5a** (1.0 g, 3.92 mmol) in THF (20 mL) at 0 °C, and the reaction mixture was stirred at 0 °C for 30 min. After addition of sodium carbonate decahydrate (2.62 g), the mixture was stirred for 1 h and the resulting mixture was filtrated through a pad of Celite® with THF. The filtrate was concentrated in vacuo, and the residue was purified by column chromatography (*n*-Hexane/EtOAc = 98:2 → 34:66) to give **5b** (850 mg, 100%) as colorless oil.

(Method B: **3b′** → **5b**+**4b**)

To a solution of **3b′** (500 mg, 1.59 mmol) in toluene (10 mL) was added dropwise 1.1 M diethylzinc in toluene (2.90 mL, 3.19 mmol) at −40 °C, and the reaction mixture was stirred at the same temperature for 30 min. After addition of diiodomethane (1.70 g, 6.36 mmol) in toluene (5 mL), the reaction mixture was stirred at 0 °C for 1 h and at room temperature for 2 h. The mixture was partitioned between water (30 mL) and EtOAc (30 mL). The organic layer was dried over $MgSO_4$, and concentrated in vacuo. The residue was purified by column chromatography (*n* Hexane/EtOAc = 100:0 → 50:50) to give *tert*-butyl(3*R*)-3-({[*tert*-butyl(dimethyl)silyl]oxy}methyl)-2-azabicyclo[3.1.0]hexane-2-carboxylate (380 mg) as colorless oil. To a solution of the above compound (380 mg) in THF (30 mL) was added 1.0 M tetra-*n*-butylammonium fluoride in THF (4.0 mL, 4.0 mmol), and the reaction mixture was stirred at room temperature for 30 min. The mixture was partitioned between water (40 mL) and EtOAc (40 mL), and the organic layer was dried over $MgSO_4$, and concentrated in vacuo. The residue was purified by column chromatography (*n*-Hexane/EtOAc = 98:2 → 34:66) to give a mixture of **5b** and **4b** (230 mg, 68%) (**5b**/**4b** = 5:1) as colorless oil.

5b: ^{1}H NMR (300 MHz, $CDCl_3$) δ 0.41 (1H, td, J = 5.2, 2.4 Hz), 0.73 (1H, br s), 1.43–1.53 (1H, m), 1.49 (9H, s), 1.68–1.92 (1H, m), 2.15 (1H, dd, J = 13.1, 8.2 Hz), 3.26 (1H, td, J = 6.2, 2.4 Hz), 3.51–3.79 (3H, m), 4.86 (1H, br s).

4.8. *tert*-Butyl(1*R*,3*R*,5*R*)-3-[(benzylamino)methyl]-2-azabicyclo[3.1.0]hexane-2-carboxylate (4c)

To a solution of **4b** (4.27 g, 20.02 mmol) and triethylamine (11.2 mL, 80.08 mmol) in DMSO (4 mL) and EtOAc (16 mL) was added dropwise a solution of sulfur trioxide pyridine complex (7.97 g, 50.05 mmol) in DMSO (28 mL) at 0 °C. The reaction mixture was stirred at 0 °C for 30 min and at room temperature for 30 min. To the reaction mixture was added 1 M HCl (80 mL, 80 mmol), and the mixture was partitioned between water (20 mL) and EtOAc (100 mL). The organic layer was washed with water (100 mL), dried over $MgSO_4$ and concentrated in vacuo. The residue was dissolved in THF (100 mL), and to the solution were added benzylamine (2.36 g, 22.02 mmol) and sodium triacetoxyborohydride (6.36 g, 30.03 mmol), successively. After stirring at room temperature for 1.5 h, the mixture was partitioned between water (100 mL) and EtOAc (100 mL). The organic layer was dried over $MgSO_4$, and concentrated in vacuo. The residue was purified by column chromatography (*n*-Hexane/EtOAc = 100:0 → 0:100) to give **4c** (5.14 g, 85%) as dark-brown solid.

^{1}H NMR (300 MHz, $CDCl_3$) δ 0.28–0.59 (1H, m), 0.63–0.80 (1H, m), 1.30–1.60 (10H, m), 1.64–1.95 (1H, m), 2.33–2.53 (1H, m), 2.64–2.83 (1H, m), 3.32–4.42 (4H, m), 5.32 (2H, s), 7.19–7.41 (5H, m).

4.9. *tert*-Butyl(1*S*,3*R*,5*S*)-3-[(benzylamino)methyl]-2-azabicyclo[3.1.0]hexane-2-carboxylate (5c)

To a mixture of **5b** (850 mg, 3.99 mmol) and triethylamine (1.59 g, 15.71 mmol) in DMSO (1.5 mL) and EtOAc (6.0 mL) was added dropwise a solution of sulfur trioxide pyridine complex (1.60 g, 10.05 mmol) in DMSO (10.5 mL) at 0 °C. The reaction mixture was stirred at 0 °C for 30 min and at room temperature for 1 h. To the reaction mixture was added 1 M HCl (15.7 mL, 15.7 mmol), and the mixture was partitioned between water (20 mL) and EtOAc (50 mL). The organic layer was washed with water (80 mL), dried over $MgSO_4$ and concentrated in vacuo. The residue was dissolved in THF (15 mL), and to the solution were added benzylamine (462 mg, 4.31 mmol) and sodium triacetoxyborohydride (1.25 g, 5.90 mmol), successively. The mixture was stirred at room temperature for 18 h, and partitioned between water (30 mL) and EtOAc (30 mL). The organic layer was dried over $MgSO_4$, and concentrated in vacuo. The residue was purified by column chromatography (*n*-Hexane/EtOAc = 75:25 → 0:100) to give **5c** (700 mg, 58%) as pale yellow solid.

^{1}H NMR (300 MHz, $CDCl_3$) δ 0.31–0.43 (1H, m), 0.75 (1H, br s), 1.30–1.57 (10H, m), 1.83–2.06 (1H, m), 2.07–2.23 (1H, m), 2.71–2.84 (1H, m), 2.93 (1H, br s), 3.08–3.31 (1H, m), 3.78–3.91 (2H, m), 3.92–4.12 (1H, m), 4.80 (1H, br s), 7.18–7.41 (5H, m).

4.10. 5-*tert*-Butyl 4-methyl (1*aR*,4*S*,6*aR*,7*aR*)-octahydro-5*H*-cyclopropa[4,5]pyrrolo[1,2-*a*]pyrazine-4,5-dicarboxylate (6)

(Method A: **8a** → **6**)

A mixture of **8a** (810 mg, 2.73 mmol) and 10% palladium on carbon (50 mg, 50% wet) in 5% HCl in MeOH (25 mL) was stirred at room temperature under hydrogen atmosphere (1 atm) for 2 h. After addition of 10% palladium on carbon (260 mg, 50% wet), the resulting mixture was further stirred at room temperature under hydrogen atmosphere (1 atm) for 5 h. The reaction mixture was filtered through a pad of Celite® with MeOH, and the filtrate was concentrated in vacuo. The residue was dissolved in THF (50 mL), and to the solution were added satd $NaHCO_3$ (50 mL) and Boc_2O (618 mg, 2.83 mmol). After stirring at room temperature for 18 h, the mixture was partitioned between water (40 mL) and EtOAc (70 mL). The organic layer was dried over $MgSO_4$, and concentrated in vacuo. The residue was purified by column chromatography (*n*-Hexane/EtOAc = 98:2 → 34:66) to give **6** (691 mg, 85%) as colorless solid.

(Method B: **8c** → **6**)

A mixture of **8c** (1.06 g, 3.58 mmol) and sodium methoxide (41 mg, 0.758 mmol) in MeOH (15 mL) was stirred at 60 °C for 1 h. After addition of sodium methoxide (150 mg, 2.78 mmol), the mixture was further stirred at 60 °C for 3 h. The mixture was partitioned between water (30 mL) and EtOAc (30 mL). The organic layer was dried over $MgSO_4$, and concentrated in vacuo. The residue was purified by column chromatography (*n*-Hexane/EtOAc = 97:3 → 34:66) to give **6** (280 mg, 26%) as colorless solid.

^{1}H NMR (300 MHz, $CDCl_3$) δ 0.38–0.52 (1H, m), 0.62–0.76 (1H, m), 1.14–1.33 (1H, m), 1.35–1.51 (10H, m), 2.04–2.25 (1H, m), 2.36–2.53 (1H, m), 2.55–3.16 (3H, m), 3.45–3.69 (1H, m), 3.69–3.94 (1H, m), 3.70–3.80 (3H, m), 4.45–4.75 (1H, m).

4.11. 5-*tert*-Butyl 4-methyl (1*aS*,4*S*,6*aR*,7*aS*)-octahydro-5*H*-cyclopropa[4,5]pyrrolo[1,2-*a*]pyrazine-4,5-dicarboxylate (7)

(Method A: **9a** → **7**)

A mixture of **9a** (220 mg, 0.742 mmol) and 10% palladium on carbon (150 mg, 50% wet) in 5% HCl in MeOH (10 mL) was stirred at room temperature for 3 h under hydrogen atmosphere (1 atm). The mixture was filtered through a pad of Celite® with MeOH, and the filtrate was concentrated in vacuo. The residue was dissolved in THF (10 mL), and to the solution were added satd $NaHCO_3$ (10 mL) and Boc_2O (168 mg, 0.77 mmol). The mixture was stirred at room temperature for 18 h, and the mixture was partitioned between water (30 mL) and EtOAc (25 mL). The organic layer was

dried over $MgSO_4$, and concentrated in vacuo. The residue was purified by column chromatography (*n*-Hexane/EtOAc = 98:2 → 34:66) to give **7** (190 mg, 86%) as colorless oil.

(Method B: **9c** → **7**)

To a solution of **9c** (240 mg, 0.810 mmol) in MeOH (4.0 mL) was added 28% sodium methoxide methanol solution (50 mg), and the reaction mixture was stirred at 60 °C for 18 h. The mixture was concentrated in vacuo, and the residue was purified by column chromatography (*n*-Hexane/EtOAc = 98:2 → 34:66) to give 7 (149 mg, 62%) as colorless oil.1H-NMR (300 MHz, $CDCl_3$) δ 0.05 (1H, dt, J = 8.1, 6.0 Hz), 0.77–0.90 (1H, m), 1.26–1.38 (1H, m), 1.38–1.50 (9H, m), 1.48–1.69 (1H, m), 1.75–1.95 (2H, m), 2.51 (1H, ddd, J = 11.1, 4.3, 2.2 Hz), 2.60–2.90 (2H, m), 3.50–3.64 (1H, m), 3.69–3.81 (3H, m), 3.81–4.07 (1H, m), 4.54–4.82 (1H, m).

4.12. Methyl(1*aR*,4*S*,6*aR*,7*aR*)-5-benzyloctahydro-1*H*-cyclopropa[4,5]pyrrolo[1,2-*a*]pyrazine-4-carboxylate (8a) and methyl (1*aR*,4*R*,6*aR*,7*aR*)-5-benzyloctahydro-1*H*-cyclopropa[4,5] pyrrolo[1,2-*a*]pyrazine-4-carboxylate (8b)

To a solution of **4c** (5.14 g, 17.00 mmol) in EtOAc (50 mL) was added 4 M HCl in EtOAc (50 mL), and the reaction mixture was stirred at room temperature for 18 h. The mixture was concentrated in vacuo, and the residue was filtered through a column of Amberlyst® A-21 (350 g, washed with methanol) with MeOH, and the filtrate was concentrated in vacuo to give 1-[(1*R*,3*R*,5*R*)-2-azabicyclo[3.1.0]hex-3-yl]-*N*-benzylmethanamine **4A** (2.76 g) as dark-brown oil. The crude product was used without further purification for the next step. To a solution of the above crude product (2.76 g) and triethylamine (5.78 mL, 41.2 mmol) in toluene (100 mL) was added methyl 2,3-dibromopropioate (3.37 g, 13.7 mmol), and the reaction mixture was stirred at 90 °C for 18 h. The mixture was partitioned between water (150 mL) and EtOAc (120 mL), and the organic layer was dried over $MgSO_4$, and concentrated in vacuo. The residue was purified by column chromatography (*n*-Hexane/EtOAc = 98:2 → 50:50) to give **8a** (810 mg, 21%, pale yellow oil) and **8b** (1.38 g, 35%, pale yellow oil).

8a: ^{1}H NMR (600 MHz, $CDCl_3$) δ 0.43–0.51 (1H, m), 0.57–0.63 (1H, m), 1.14–1.30 (1H, m), 1.32–1.40 (1H, m), 1.99–2.11 (1H, m), 2.37–2.43 (1H, m), 2.49 (1H, dd, J = 11.0, 3.9 Hz), 2.70 (1H, t, J = 11.0 Hz), 2.99 (1H, dd, J = 11.4, 4.0 Hz), 3.10–3.17 (1H, m), 3.33–3.41 (1H, m), 3.55 (1H, dd, J = 11.4, 2.2 Hz), 3.71 (3H, s), 3.85–3.96 (2H, m), 7.23 (1H, t, J = 6.8 Hz), 7.27–7.34 (4H, m).

^{13}C NMR (151 MHz, $CDCl_3$) δ 15.2, 21.1, 32.8, 43.1, 51.2, 52.1, 52.3, 59.2, 60.0, 66.9, 126.9, 128.2 (2C), 128.6 (2C), 139.4, 173.1.

8b: ^{1}H NMR (600 MHz, $CDCl_3$) δ 0.53–0.70 (2H, m), 1.34–1.43 (1H, m), 1.73 (1H, t, J = 11.2 Hz), 2.10 (1H, ddd, J = 13.1, 7.0, 6.7 Hz), 2.47–2.58 (1H, m), 2.65 (1H, dd, J = 11.4, 3.7 Hz), 2.99 (1H, t, J = 11.0 Hz), 3.17–3.26 (4H, m), 3.36 (1H, dd, J = 11.6, 3.5 Hz), 3.76 (3H, s), 3.82 (1H, d, J = 12.8 Hz), 7.22–7.27 (1H, m), 7.28–7.35 (4H, m).

^{13}C NMR (151 MHz, $CDCl_3$) δ 15.0, 20.0, 32.6, 43.2, 52.1 (2C), 56.0, 60.5 (2C), 64.2, 127.3, 128.2 (2C), 129.5 (2C), 137.0, 173.2.

4.13. 5-*tert*-Butyl 4-methyl (1*aR*,4*R*,6*aR*,7*aR*)-octahydro-5*H*-cyclopropa[4,5]pyrrolo[1,2-*a*]pyrazine-4,5-dicarboxylate (8c)

A mixture of **8b** (1.38 g, 4.75 mmol) and 10% palladium on carbon (500 mg, 50% wet) in 5% HCl in MeOH (20 mL) was stirred at room temperature under hydrogen atmosphere (1 atm) for 5 h. The reaction mixture was filtered through a pad of Celite® with MeOH, and the filtrate was concentrated in vacuo. The residue was dissolved in THF (50 mL), and to the solution were added satd $NaHCO_3$ (50 mL) and Boc_2O (1.04 g, 4.76 mmol). After stirring at room temperature for 18 h, the mixture was partitioned between water (30 mL) and EtOAc (70 mL). The organic layer was dried over $MgSO_4$, concentrated in vacuo and the residue was purified by column chromatography (*n*-Hexane/EtOAc = 98:2 → 34:66) to give **8c** (1.06 g, 75%) as pale yellow solid.

^{1}H NMR (300 MHz, $CDCl_3$) δ 0.32–0.50 (2H, m), 1.33–1.63 (11H, m), 2.35–2.51 (1H, m), 2.72–2.97 (2H, m), 3.05–3.16 (1H, m), 3.28–3.51 (1H, m), 3.55–3.86 (4H, m), 3.86–4.01 (1H, m), 4.34–4.54 (1H, m).

4.14. Methyl(1*aS*,4*R*,6*aR*,7*aS*)-5-benzyloctahydro-1*H*-cyclopropa[4,5]pyrrolo[1,2-*a*]pyrazine-4-carboxylate (9a) and methyl (1a*S*,4*S*,6a*R*,7a*S*)-5-benzyloctahydro-1*H*-cyclopropa[4,5]pyrrolo[1,2-a]pyrazine-4-carboxylate (9b)

To a solution of **5c** (700 mg, 2.31 mmol) in EtOAc (10 mL) was added 4 M HCl in EtOAc (30 mL, 120 mmol), and the reaction mixture was stirred at room temperature for 3 h. The reaction mixture was concentrated in vacuo, the precipitated solid was collected by filtration, and dissolved in toluene (30 mL). To the solution were added methyl 2,3-dibromopropionate (512 mg, 2.08 mmol) and triethylamine (4.62 mL, 33.15 mmol), and the reaction mixture was stirred at 90 °C for 18 h. The mixture was partitioned between water (50 mL) and EtOAc (50 mL), and the organic layer was dried over $MgSO_4$, and concentrated in vacuo. The residue was purified by column chromatography (*n*-Hexane/EtOAc = 75:25 → 0:100) to give **9a** (45 mg, 8%, pale yellow oil) and **9b** (290 mg, 49%, colorless oil).

9a: ^{1}H NMR (600 MHz, $CDCl_3$) δ −0.04–0.07 (1H, m), 0.81–0.97 (1H, m), 1.25–1.34 (1H, m), 1.57 (1H, td, J = 11.5, 4.6 Hz), 1.77 (1H, dd, J = 11.5, 6.1 Hz), 2.01–2.14 (1H, m), 2.58–2.71 (3H, m), 2.88 (1H, t, J = 10.1 Hz), 3.34–3.45 (1H, m), 3.48 (1H, br s), 3.73 (3H, s), 3.83–4.00 (2H, m), 7.18–7.24 (1H, m), 7.29 (4H, d, J = 4.4 Hz).

^{13}C NMR (151 MHz, $CDCl_3$) δ 1.7, 12.3, 29.9, 40.3, 51.2 (2C), 53.0, 55.8, 59.0, 60.3, 126.9, 128.2 (2C), 128.6 (2C), 139.4, 173.0.

9b: ^{1}H NMR (600 MHz, $CDCl_3$) δ −0.03–0.10 (1H, m), 0.84–0.92 (1H, m), 1.30–1.38 (1H, m), 1.53 (1H, td, J = 11.4, 4.4 Hz), 1.78 (1H, dd, J = 11.4, 6.1 Hz), 1.88 (1H, t, J = 10.3 Hz), 2.04–2.13 (1H, m), 2.59 (1H, t, J = 10.3 Hz), 2.69 (1H, dt, J = 5.9, 2.6 Hz), 2.90 (1H, dd, J = 10.3, 2.6 Hz), 3.24–3.29 (2H, m), 3.31 (1H, dd, J = 10.3, 3.7 Hz), 3.77 (3H, s), 3.80–3.87 (1H, m), 7.23–7.28 (1H, m), 7.29–7.34 (4H, m).

^{13}C NMR (151 MHz, $CDCl_3$) δ 2.1, 12.1, 29.9, 40.0, 52.1, 53.0, 54.4, 54.6, 60.5, 65.2, 127.3, 128.2 (2C), 129.6 (2C), 137.0, 172.9.

4.15. 5-*tert*-Butyl 4-methyl (1*aS*,4*R*,6*aR*,7*aS*)-octahydro-5*H*-cyclopropa[4,5]pyrrolo[1,2-*a*]pyrazine-4,5-dicarboxylate (9c)

A mixture of **9b** (290 mg, 1.01 mmol) and 10% palladium on carbon (150 mg, 50% wet) in 5% HCl in MeOH (5.0 mL) was stirred at room temperature for 8 h under hydrogen atmosphere (1 atm). The mixture was filtered through a pad of Celite® with MeOH, and the filtrate was concentrated in vacuo. The residue was dissolved in THF (10 mL), and to the solution were added satd $NaHCO_3$ (10 mL) and Boc_2O (218 mg, 1.0 mmol). The mixture was stirred at room temperature for 18 h, and partitioned between water (25 mL) and EtOAc (40 mL). The organic layer was dried over $MgSO_4$, and concentrated in vacuo. The residue was purified by column chromatography (*n*-Hexane/EtOAc = 97:3 → 33:67) to give **9c** (240 mg, 80%) as colorless oil.

^{1}H NMR (300 MHz, $CDCl_3$) δ 0.22–0.36 (1H, m), 0.77 (1H, dd, J = 3.8, 2.6 Hz), 1.34–1.49 (10H, m), 1.72 (2H, d, J = 8.3 Hz), 2.48 (1H, br s), 2.53–2.66 (1H, m), 2.82–3.04 (2H, m), 3.36 (1H, dd, J = 12.8, 4.7 Hz), 3.68 (1H, dd, J = 13.0, 3.6 Hz), 3.72–3.80 (3H, m), 4.39 (1H, br s).

4.16. *tert*-Butyl(1*aR*,4*S*,6*aR*,7*aR*)-4-[(4*R*)-3,4-dihydro-2*H*-chromen-4-ylcarbamoyl]octahydro-5*H*-cyclopropa[4,5]pyrrolo[1,2-*a*]pyrazine-5-carboxylate (11)

To a solution of **6** (691 mg, 2.33 mmol) in THF (5 mL) were added lithium hydroxide monohydrate (202 mg, 4.81 mmol) and water (1.5 mL). After stirring at 50 °C for 5 h, the reaction mixture was neutralized with 1 M HCl (4.8 mL), and concentrated in vacuo. The residue was dissolved in DMF (120 mL), and to the solution were added (*R*)-chroman-4-amine hydrochloride **10** (650 mg, 3.50 mmol), 1-hydroxybenzotriazole (315 mg, 2.33 mmol), DIPEA (0.81 mL, 4.66 mmol) and WSC (2.95 g, 15.38 mmol) successively. The reaction mixture was stirred at room temperature for 18 h, and partitioned between water (150 mL) and EtOAc (150 mL). The organic layer was washed with satd $NaHCO_3$ (150 mL), brine (100 mL), dried over $MgSO_4$ and concentrated in vacuo. The residue was purified by column chromatography (*n*-Hexane/EtOAc = 91:9 → 0:100) to give **11** (172 mg, 18%) as colorless oil.

^{1}H NMR (300 MHz, $CDCl_3$) δ 0.27–0.49 (1H, m), 0.68–0.78 (1H, m), 1.10–1.70 (2H, m), 1.44 (9H, s), 1.91–2.08 (1H, m), 2.13–2.29 (2H, m), 2.45–2.68 (2H, m), 2.76–2.88 (1H, m), 2.97–3.11 (1H, m), 3.45–4.21 (3H, m), 4.19–4.31 (1H, m), 4.49–4.74 (1H, m), 5.12–5.26 (1H, m), 6.43–6.76 (1H, m), 6.79–6.96 (2H, m), 7.13–7.25 (2H, m).

4.17. *tert*-Butyl(1*aS*,4*S*,6*aR*,7*aS*)-4-[(4*R*)-3,4-dihydro-2*H*-chromen-4-ylcarbamoyl]octahydro-5*H*-cyclopropa[4,5]pyrrolo[1,2-*a*]pyrazine-5-carboxylate (12)

A mixture of **7** (240 mg, 0.652 mmol) and lithium hydroxide monohydrate (60.3 mg, 1.44 mmol) in THF (4 mL) and water (1.0 mL) was stirred at 50 °C for 4 h. The reaction mixture was concentrated in vacuo, and the residue was dissolved in DMF (10 mL). To the solution were added (*R*)-chroman-4-amine hydrochloride **10** (200 mg, 1.34 mmol), DIPEA (280 mg, 2.17 mmol) and HATU (683 mg, 1.80 mmol) successively. The reaction mixture was stirred at room temperature for 18 h, and the mixture was partitioned between water (15 mL) and EtOAc (15 mL). The organic layer was washed with satd $NaHCO_3$ (20 mL) and brine (20 mL), dried over $MgSO_4$ and concentrated in vacuo. The residue was purified by column chromatography (*n*-Hexane/EtOAc = 98:2 → 20:80) to give **12** (254 mg, 94%) as colorless amorphous solid.

^{1}H NMR (300 MHz, $CDCl_3$) δ 0.08 (1H, dt, J = 8.1, 6.0 Hz), 0.78–0.86 (1H, m), 1.31–1.48 (10H, m), 1.49–1.63 (1H, m), 1.82–2.10 (2H, m), 2.14–2.33 (1H, m), 2.39–2.49 (1H, m), 2.50–2.84 (2H, m), 3.69–3.85 (1H, m), 3.93–4.32 (3H, m), 4.58–4.83 (1H, m), 5.14–5.26 (1H, m), 6.30–6.57 (1H, m), 6.78–6.95 (2H, m), 7.14–7.27 (3H, m).

4.18. *tert*-Butyl[(1*S*)-1-cyclohexyl-2-{(1*aR*,4*S*,6*aR*,7*aR*)-4-[(4*R*)-3,4-dihydro-2*H*-chromen-4-ylcarbamoyl]octahydro-5*H*-cyclopropa[4,5]pyrrolo[1,2-*a*]pyrazin-5-yl}-2-oxoethyl]carbamate (14)

To a solution of **11** (172 mg, 0.416 mmol) in EtOAc (20 mL) was added 4 M HCl in EtOAc (30 mL, 120 mmol), and the mixture was stirred at room temperature for 2 h. The reaction mixture was concentrated in vacuo, and the residue was dissolved in DMF (5 mL). To the solution were added (2*S*)-[(*tert*-butoxycarbonyl)amino](cyclohexyl)ethanoic acid **13** (139 mg, 0.540 mmol), DIPEA (270 mg, 0.540 mmol) and HATU (240 mg, 0.631 mmol) successively, and the resulting mixture was stirred at room temperature for 48 h. The mixture was partitioned between water (20 mL) and EtOAc (25 mL), and the organic layer was washed with satd $NaHCO_3$ (25 mL) and brine (25 mL), and concentrated in vacuo. The residue was purified by column chromatography (*n*-Hexane/EtOAc = 25:75 → 0:100, EtOAc/MeOH = 100:0 → 66:34) to give **14** (182 mg, 79%) as colorless amorphous solid.

^{1}H NMR (300 MHz, DMSO-d_6) δ 0.35–0.51 (1H, m), 0.47–0.65 (1H, m), 0.81–3.48 (21H, m), 1.20–1.44 (9H, m), 3.65–3.95 (1H, m), 4.07–4.33 (3H, m), 4.48–4.68 (1H, m), 4.90–5.06 (1H, m), 6.63–6.91 (3H, m), 7.05–7.33 (2H, m), 8.16–8.36 (1H, m).

4.19. *tert*-Butyl[(1*S*)-1-cyclohexyl-2-{(1*aS*,4*S*,6*aR*,7*aS*)-4-[(4*R*)-3,4-dihydro-2*H*-chromen-4-ylcarbamoyl]octahydro-5*H*-cyclopropa[4,5]pyrrolo[1,2-*a*]pyrazin-5-yl}-2-oxoethyl]carbamate (15)

To a solution of **12** (254 mg, 0.61 mmol) in MeOH (10 mL) was added 4 M HCl in EtOAc (20 mL, 80 mmol), and the reaction mixture was stirred at room temperature for 3 h. After concentration of the reaction mixture, the precipitated solid was collected by filtration, washed with *i*-Pr_2O (25 mL) and EtOAc (10 mL). The collected solid was dissolved in DMF (10 mL), and to the solution were added (2*S*)-[(*tert*-butoxycarbonyl)amino](cyclohexyl)ethanoic acid **13** (205 mg, 0.797 mmol), DIPEA (397 mg, 3.07 mmol) and HATU (397 mg, 1.04 mmol) successively. The reaction mixture was stirred at room temperature for 1 h, and partitioned between water (25 mL) and EtOAc (25 mL). The organic layer was washed with satd $NaHCO_3$ (25 mL), brine (25 mL), dried over $MgSO_4$ and concentrated in vacuo. The residue was purified by column chromatography (*n*-Hexane/EtOAc = 91:9 → 20:80) to give **15** (250 mg, 74%) as colorless oil.

^{1}H NMR (300 MHz, $CDCl_3$) δ 0.03–0.16 (1H, m), 0.45–3.13 (31H, m), 3.68–5.40 (7H, m), 6.14–7.71 (5H, m).

4.20. *tert*-Butyl[(1*S*)-2-{[(1*S*)-1-cyclohexyl-2-{(1*aR*,4*S*,6*aR*,7*aR*)-4-[(4*R*)-3,4-dihydro-2*H*-chromen-4-ylcarbamoyl]octahydro-5*H*-cyclopropa[4,5]pyrrolo[1,2-*a*]pyrazin-5-yl}-2-oxoethyl]amino}-1-methyl-2-oxoethyl]methylcarbamate (17)

To a solution of **14** (182 mg, 0.329 mmol) in EtOAc (10 mL) was added 4 M HCl in EtOAc (20 mL, 80 mmol), and the reaction mixture was stirred at room temperature for 1.5 h. The reaction mixture was concentrated in vacuo, and the residue was dissolved in DMF (5 mL). To the solution were added *N*-(*tert*-butoxycarbonyl)-*N*-methyl-L-alanine **16** (80 mg, 0.394 mmol), DIPEA (0.385 mL, 2.21 mmol) and HATU (187 mg, 0.492 mmol) successively, and the reaction mixture was stirred at room temperature for 1.5 h. The mixture was partitioned between water (25 mL) and EtOAc (25 mL), and the organic layer was washed with satd $NaHCO_3$ (25 mL), brine (25 mL), dried over $MgSO_4$ and concentrated in vacuo. The residue was purified by column chromatography (*n*-Hexane/EtOAc = 25:75 → 0:100, EtOAc/MeOH = 100:0 → 50:50) to give **17** (77.1 mg, 37%) as colorless amorphous solid.

^{1}H NMR (300 MHz, $CDCl_3$) δ 0.34–0.47 (1H, m), 0.66–0.87 (1H, m), 0.81–3.27 (36H, m), 3.47–5.23 (7H, m), 6.49–8.08 (6H, m).

4.21. *tert*-Butyl[(1*S*)-2-{[(1*S*)-1-cyclohexyl-2-{(1*aS*,4*S*,6*aR*,7*aS*)-4-[(4*R*)-3,4-dihydro-2*H*-chromen-4-ylcarbamoyl]octahydro-5*H*-cyclopropa[4,5]pyrrolo[1,2-*a*]pyrazin-5-yl}-2-oxoethyl]amino}-1-methyl-2-oxoethyl]methylcarbamate (18)

To a solution of **15** (250 mg, 0.392 mmol) in EtOAc (10 mL) was added 4 M HCl in EtOAc (20 mL, 80 mmol), and the reaction mixture was stirred at room temperature for 3.5 h. The reaction mixture was concentrated in vacuo, and the precipitated solid was collected by filtration, washed with *i*-Pr_2O (20 mL) and EtOAc (10 mL). The obtained solid was dissolved in DMF (5.0 mL), and to the solution were added *N*-(*tert*-butoxycarbonyl)-*N*-methyl-L-alanine **16** (120 mg, 0.59 mmol), DIPEA (293 mg, 2.27 mmol) and HATU (260 mg, 0.684 mmol) successively. The reaction mixture

was stirred at room temperature for 3 h, and partitioned between water (20 mL) and EtOAc (20 mL). The organic layer was washed with satd $NaHCO_3$ (20 mL), brine (20 mL), dried over $MgSO_4$ and concentrated in vacuo. The residue was purified by column chromatography (*n*-Hexane/EtOAc = 9:91 → 20:80) to give **18** (220 mg, 82%) as colorless amorphous powder.

^{1}H NMR (300 MHz, $CDCl_3$) δ 0.03−0.19 (1H, m), 0.45−3.08 (37H, m), 3.73−5.31 (7H, m), 6.13−7.62 (6H, m).

4.22. Calculations for thermodynamic stability of 6, 7, 8c and 9c

The conformations of **6**, **7**, **8c** and **9c** were generated by Omega2 and geometrically optimized by MultiMinimization function of Macromodel where MMFF94s as the force field, 80 as the dielectric constant, and GB/SA for the solvation model were used, respectively.

4.23. Preparations of proteins, peptides and reagents

The recombinant BIR3 domain (residues 250–350) of human cIAP1 protein fused to His-tag (cIAP_BIR3) was prepared in Discovery Research Center. The *N*-terminal His-tagged BIR3 domain (residues 252–356) of recombinant human XIAP protein (XIAP_BIR3) and Smac-N7 peptide (AVPIAQK; Smac-N7) were purchased from R&D Systems, Inc., and EMD Chemicals Inc. (Calbiochem), respectively. A C-terminally biotinated Smac-N7 peptide (AVPIAQ-K(biotin)-NH_2; biotinyl-Smac) was synthesized at Peptide Institute Inc. Europium cryptate (Eu^{3+} cryptate)-conjugated mouse monoclonal antibody anti-6-Histidine (Anti-6HIS Cryptate), high grade XL665-conjugated streptavidin (SA-XL$^{ent!}$), and HTRF detection buffer were purchased from Sceti Medical Labo K.K. (cisbio). Anti-6HIS Cryptate and SA-XL$^{ent!}$ were dissolved in distillated water, and stored at −30 °C, according to the manufacture's protocol. Other reagents used were obtained from Wako Pure Chemicals and were of analytical grade or comparable.

4.24. Binding activities using homogeneous time-resolved fluorescence resonance energy transfer (HTRF) technology

Binding experiments were performed in white low-volume 384-well plates (Greiner, #784075). A 5 μL of IAP proteins (40 nM for XIAP_BIR3, 8 nM for cIAP_BIR3) and 5 μL of increasing concentration of compounds were added to wells in the assay buffer (25 mM HEPES, 100 mM NaCl, 0.1% BSA, 0.1% Triton X-100, pH 7.5). After shaking at room temperature, 5 μL of biotinyl-Smac (20 nM for XIAP_BIR3 and 80 nM for cIAP_BIR3, dissolved in assay buffer) added to the well, followed by adding 5 μL of mixture of Anti-6HIS Cryptate and SA-XL$^{ent!}$, 100 times diluted with HTRF detection buffer, respectively. In some case, the condition of 40 nM cIAP_BIR3 and 20 nM biotinyl-Smac was used for the compound evaluation.

After overnight incubation at room temperature in the dark, HTRF measurement was carried out on a multi-label reader (EnVision, PerkinElmer Life And Analytical Sciences, Inc.) with the following settings:

Measurement mode: time-resolved fluorescence.
Excitation: 320 nm.
Emission donor: 615 nm.
Emission acceptor: 665 nm.
Measurement height: 6.5 mm.
Cycle: 2000.
Delay: 90 ms.
Number of flashes: 280 μs.

Fluorescence collected at 615 nm (F_{615nm}) is the total europium cryptate signal, and fluorescence collected at 665 nm (F_{665nm}) is the FRET signal. The ratio = (F_{665nm}/F_{615nm}) × 10,000 was calculated and IC_{50} values were determined using the ratio by nonlinear regression curve fitting with the program Prism (GraphPad Software).

4.25. Preparation of cell lines

For in vitro assay, MDA-MB-231 breast cancer cell line and MRC5 normal lung fibroblast were obtained from ATCC. The culture medium recommended by suppliers was used for cultivation of each cell line. For in vivo study, MDA-MB-231-Luc cells were established at Takeda Pharmaceutical Company Ltd. (TPC) (Fujisawa, Kanagawa, Japan) by transfecting firefly luciferase expression vector (Promega Corp., Madison, WI USA) into MDA-MB-231 cells.

4.26. Measurement of cell viability

MDA-MB-231 cells were seeded in triplicate 96-well plates in 100 μL complete media at a density of 3×10^3 cells/well. Compounds were added to each well to give a range of concentrations (0.0001–0.1 μM) in a final volume of 200 μL. Cell viability was measured using CellTiter-Glo® Luminescent Cell Viability Assay (Promega) at 72 h of incubation.

4.27. In vivo PD study

Eight-week-old mice were inoculated SC with 5×10^6 MDA-MB-231-Luc cells when tumors had grown to approximately 200 mm^3, the mice were dosed administrated orally with 20, 100 mg/kg of **2** in 10% methylcellulose. Mice were euthanized and tumors were harvested at 6 h after dosing. Pharmacodynamics of compounds was assessed by measuring tumor TNF alpha mRNA level.

4.28. Real-time reverse transcription PCR

Total ribonucleic acid (RNA) samples from tumor tissues were purified using the RNeasy mini kit (Qiagen, Tokyo, Japan). First strand complementary deoxyribonucleic acid (cDNA) was synthesized from total RNA using the Reverse transcription reagents (Applied Biosystems, Inc.). The amount of human TNF alpha and GAPDH cDNA in each sample was measured by qPCR using the 7900HT real-time PCR system with TaqMan primer/probe set and Universal PCR MasterMix (Applied Biosystems, Inc.). The amount of human TNF alpha mRNA in each sample was quantified and normalized as follows. The cycle threshold (Ct) of human TNF alpha was subtracted from Ct of human TNF alpha to calculated ΔCT value (Ct (TNF alpha)-Ct (GAPDH)). Relative fold difference was expressed as a power of 2 (2-CT (TNF alpha)-Ct (GAPDH)).

4.29. Metabolic stability assay

Human and mouse hepatic microsomes were purchased from Xenotech, LLC (Lenexa, KS). An incubation mixture with a final volume of 50 μL consisted of microsomal protein in 50 mmol/L phosphate buffer (pH 7.4) and 1 μmol/L test compound. The concentration of microsomal protein was 0.2 mg/mL. An NADPH-generating system containing 25 mmol/L $MgCl_2$, 25 mmol/L glucose-6-phosphate, 2.5 mmol/L β-$NADP^+$ and 7.5 unit/mL glucose-6-phosphate dehydrogenase was added to the incubation mixture with a 20% volume of the reaction mixture to initiate the enzyme reaction. After the addition of the NADPH-generating system, the mixture was incubated at 37 °C for 15 and 30 min. The reaction was terminated by the addition of acetonitrile equivalent to the volume of the reaction mixture. All incubations were made in duplicate. The test compound in the reaction mixture was measured by LC/MS/MS analysis. For metabolic stability determinations, chromatograms were analyzed for parent compound disappearance from the reaction mixtures.

4.30. X-ray structure analysis of compound 12

All measurements were made on a Rigaku R-AXIS RAPID diffractometer using graphite monochromated Cu-K_α radiation. The structure was solved by direct methods with SHELXS-97[28] and was refined using full-matrix least-squares on F^2 with SHELXL-97.[28] All nonH atoms were refined with anisotropic displacement parameters.

Crystal data for compound **12**: $C_{23}H_{31}N_3O_4$, MW = 413.52; crystal size, 0.21 × 0.14 × 0.09 mm; colorless, block; monoclinic, space group $P2_1$, a = 6.74880(10) Å, b = 17.2276(3) Å, c = 9.3451(2) Å, $\alpha = \gamma = 90°$, β = 93.7440(9)°, V = 1084.20(3) Å^3, Z = 2, Dx = 1.267 g/cm^3, T = 100 K, μ = 0.7065 mm^{-1}, λ = 1.54187 Å, R_1 = 0.034, wR_2 = 0.089, Flack Parameter = 0.11(16).

CCDC 938836 for compound **12** contains the Supplementary Crystallographic Data for this paper. These data can be obtained free of charge from The Cambridge Crystallographic Data Centre via www.ccdc.cam.ac.uk/data_request/cif.

4.31. cIAP Molecular biology, protein expression, purification and crystallography

The BIR3 domain of human cIAP-1 (residues 260–352) was over-expressed as 6xHis tag protein in *Escherichia coli*. The cIAP-1 protein was purified by immobilized Ni^{2+} affinity chromatography, followed by cleavage of the 6×His tag with TEV protease and size exclusion with a Superdex 200 column (GE Healthcare). The final protein buffer for the compound A/cIAP-1 complex was 25 mM TRIS pH 7.6, 50 mM NaCl, 0.25 mM TCEP and 1 mM $MgCl_2$. The compound **2**/cIAP-1 complex protein buffer was 25 mM HEPES pH 7.6, 50 mM NaCl and 1 mM $MgCl_2$. Prior to crystallization, the purified proteins were mixed with 1–3 mM inhibitor compound and concentrated to 18 mg/ml.

Crystals suitable for data collection were obtained by vapor diffusion in sitting drops at 20 °C. Reservoirs contained 2.8−3.2 M NaCl and 100 mM HEPES (pH 7.3−7.7) for the compound **A**/cIAP-1 complex. The compound **2**/cIAP-1 complex crystals formed in 2.3−2.8 M NaCl, 0.2 M $MgCl_2$ and 100 mM Tris (pH 6.8−7.2). Crystals were immersed in mother liquor solution containing 22% ethylene glycol for cryo protection and flash frozen in liquid nitrogen. Crystals of both ligand cIAP-1 complexes grew in the orthorhombic space group $P2_12_12_1$ with similar unit cell dimensions and two molecules in the asymmetric unit.

Diffraction data were collected from single cryogenically protected crystals at beamline 5.0.3 of the Advanced Light Source at Lawrence Berkeley National Laboratory. Data were reduced using the HKL2000 software package.[29] The structures were determined by molecular replacement with either MOLREP[30] or PHASER[31] of the CCP4 program suite utilizing PDB code 3D9T and refined with the program REFMAC.[32] Several cycles of model building with XtalView[33] and refinement was performed to improve the quality of the model. Data reduction and refinement statistics are summarized in Supplementary Table S1. The coordinates and structure factors have been deposited in Protein data bank and assigned the accession code 4LGU (compound **A**/cIAP-1 complex) and 4LGE (compound **2**/cIAP-1 complex).

Acknowledgments

We are grateful to the members of the structural biology group (Bi-Ching Sang, Hua Zou, Ryan D. Bertsch, and Gyorgy P. Snell) and the management at Takeda California for determining the X-ray co-crystal structure of compound **A** and **2** with cIAP-1. The authors would also like to acknowledge Motoo Iida and Mie Itou for the measurement of the X-ray single-crystal structure of compound **12**. The staff of the Berkeley Center for Structural Biology is gratefully acknowledged for support of beamline 5.0.3 at the Advanced Light Source. The Advanced Light Source is supported by the Director, Office of Science, Office of Basic Energy Sciences, of the U.S. Department of Energy under Contract No. DE-AC02-05CH11231.

Supplementary data

Supplementary data associated with this article can be found, in the online version, at http://dx.doi.org/10.1016/j.bmc.2013.07.020.

References and notes

1. Salvesen, G. S.; Duckett, C. S. *Nat. Rev. Mol. Cell Biol.* **2002**, *3*, 401.
2. Deveraux, Q. L.; Reed, J. C. *Genes Dev.* **1999**, *13*, 239.
3. Deng, Y.; Ren, X.; Yang, L.; Lin, Y.; Wu, X. *Cell* **2003**, *115*, 61.
4. Fotin-Mleczek, M.; Henkler, F.; Samel, D.; Reichwein, M.; Hausser, A.; Parmryd, I.; Scheurich, P.; Schmid, J. A.; Wajant, H. *J. Cell Sci.* **2002**, *115*, 2757.
5. Deveraux, Q. L.; Takahashi, R.; Salvesen, G. S.; Reed, J. C. *Nature* **1997**, *388*, 300.
6. Holcik, M.; Gibson, H.; Korneluk, R. G. *Apoptosis* **2001**, *6*, 253.
7. Tamm, I.; Kornblau, S. M.; Segall, H.; Krajewski, S.; Welsh, K.; Kitada, S.; Scudiero, D. A.; Tudor, G.; Qui, Y. H.; Monks, A.; Andreeff, M.; Reed, J. C. *Clin. Cancer Res.* **2000**, *6*, 1796.
8. Straub, C. S. *Curr. Top. Med. Chem.* **2011**, *11*, 291.
9. Mannhold, R.; Fulda, S.; Carosati, E. *Drug Disc. Today* **2010**, *15*, 210.
10. Du, C.; Fang, M.; Li, Y.; Li, L.; Wang, X. *Cell* **2000**, *102*, 33.
11. Varfolomeev, E.; Blankenship, J. W.; Wayson, S. M.; Fedorova, A. V.; Kayagaki, N.; Garg, P.; Zobel, K.; Dynek, J. N.; Elliott, L. O.; Wallweber, H. J.; Flygare, J. A.; Fairbrother, W. J.; Deshayes, K.; Dixit, V. M.; Vucic, D. *Cell* **2007**, *131*, 669.
12. Vince, J. E.; Wong, W. W.-L.; Khan, N.; Feltham, R.; Chau, D.; Ahmed, A. U.; Benetatos, C. A.; Chunduru, S. K.; Condon, S. M.; McKinlay, M.; Brink, R.; Leverkus, M.; Tergaonkar, V.; Schneider, P.; Callus, B. A.; Koentgen, F.; Vaux, D. L.; Silke, J. *Cell* **2007**, *131*, 682.
13. Srinivasula, S. M.; Hegde, R.; Saleh, A.; Datta, P.; Shiozaki, E.; Chai, J.; Lee, R.-A.; Robbins, P. D.; Fernandes-Alnemri, T.; Shi, Y.; Alnemri, E. S. *Nature* **2001**, *410*, 112.
14. Sun, H.; Nikolovska-Coleska, Z.; Yang, C.-Y.; Qian, D.; Lu, J.; Qiu, S.; Bai, L.; Peng, Y.; Cai, Q.; Wang, S. *Acc. Chem. Res.* **2008**, *41*, 1264.
15. Oost, T. K.; Sun, C.; Armstrong, R. C.; Al-Assaad, A.-S.; Betz, S. F.; Deckwerth, T. L.; Ding, H.; Elmore, S. W.; Meadows, R. P.; Olejniczak, E. T.; Oleksijew, A.; Oltersdorf, T.; Rosenberg, S. H.; Shoemaker, A. R.; Tomaselli, K. J.; Zou, H.; Fesik, S. W. *J. Med. Chem.* **2004**, *47*, 4417.
16. Dienstmann, R.; Vidal, L.; Dees, E. C.; Chia, S.; Mayer, E. L.; Porter, D.; Baney, T.; Dhuria, S.; Sen, S. K.; Firestone, B.; Papoutsakis, D.; Cameron, S. Abstract of papers, 35th Annual San Antonio Breast Cancer Symposium, San Antonio, TX, December 2012; Abstract 75s.
17. Flygare, J. A.; Beresini, M.; Budha, N.; Chan, H.; Chan, I. T.; Cheeti, S.; Cohen, F.; Deshayes, K.; Doerner, K.; Eckhardt, S. G.; Elliott, L. O.; Feng, B.; Franklin, M. C.; Reisner, S. F.; Gazzard, L.; Halladay, J.; Hymowitz, S. G.; La, H.; LoRusso, P.; Maurer, B.; Murray, L.; Plise, E.; Quan, C.; Stephan, J.-P.; Young, S. G.; Tom, J.; Tsui, V.; Um, J.; Varfolomeev, E.; Vucic, D.; Wagner, A. J.; Wallweber, H. J. A.; Wang, L.; Ware, J.; Wen, Z.; Wong, H.; Wong, J. M.; Wong, M.; Wong, S.; Yu, R.; Zobel, K.; Fairbrother, W. J. *J. Med. Chem.* **2012**, *55*, 4101.
18. Eckhardt, S. G.; Gallant, G.; Sikic, B. I.; Camidge, D. R.; Burris III, H. A.; Wakelee, H. A.; Messersmith, W. A.; Jones, S. F.; Colevas, A. D.; Infante, J. R. Abstract of Papers, 46th Annual Meeting of the American Society of Clinical Oncology, Chicago, IL, June 2010; Abstract 2580.
19. Condon, S. M.; Deng, Y.; Haimowitz, T.; Rippin, S. R.; LaPorte, M. G.; Alexander, M. D.; Hendi, M. S.; Lee, Y.-H.; Kumar, T. P.; Mitsuuchi, Y.; Benetatos, C. A.; McKinlay, M. A.; Kapoor, G. S.; Neiman, E. M.; Seipel, M. E.; Yu, G.; Burns, J. M.; Graham, M.; Weng, D.; Chunduru, S. K. Abstract of Papers, 245th National Meeting of the American Chemical Society, New Orleans, LA, April 2013; Abstract 279.
20. Cai, Q.; Sun, H.; Peng, Y.; Lu, J.; Nikolovska-Coleska, Z.; McEachern, D.; Liu, L.; Qiu, S.; Yang, C.-Y.; Miller, R.; Yi, H.; Zhang, T.; Sun, D.; Kang, S.; Guo, M.; Leopold, L.; Yang, D.; Wang, S. *J. Med. Chem.* **2011**, *54*, 2714.
21. Hashimoto, K.; Saito, B.; Miyamoto, N.; Oguro, Y.; Tomita, D.; Shiokawa, Z.; Asano, M.; Kakei, H.; Taya, N.; Kawasaki, M.; Sumi, H.; Yabuki, M.; Iwai, K.; Yoshida, S.; Yoshimatsu, M.; Aoyama, K.; Kosugi, Y.; Kojima, T.; Morishita, N.; Dougan, D. R.; Snell, G. P.; Imamura, S.; Ishikawa, T. *J. Med. Chem.* **2013**, *56*, 1228.
22. Sumi, H.; Yabuki, M.; Iwai, K.; Morimoto, M.; Hibino, R.; Inazuka, M.; Hashimoto, K.; Kosugi, Y.; Aoyama, K.; Yamamoto, S.; Yoshimatsu, M.; Yamasaki, H.; Tozawa, R.; Ishikawa, T.; Yoshida, S. *Mol. Cancer Ther.* **2013**, *12*, 230.
23. Lebel, H.; Marcoux, J.-F.; Molinaro, C.; Charette, A. B. *Chem. Rev.* **2003**, *103*, 977.
24. Yu, J.; Truc, V.; Riebel, P.; Hierl, E.; Mudryk, B. *Tetrahedron Lett.* **2005**, *46*, 4011.
25. Hanessian, S.; Reinhold, U.; Saulnier, M.; Claridge, S. *Bioorg. Med. Chem. Lett.* **1998**, *8*, 2123.
26. Mohapatra, D. K. *J. Chem. Soc., Perkin Trans. 1* **2001**, 1851.
27. According to 1D- and 2D-NMR (NOESY, HMBC) analyses, the *C*-4 hydrogen atom of **8a** and **9a** was supposed to be placed in an equatorial position. In addition, the *C*-4 hydrogen atom of **8b** and **9b** was suggested to be attached in an axial position.
28. Sheldrick, G. M. *Acta Crystallogr., Sect. A* **2008**, *64*, 112.

29. Otwinowski, Z.; Minor, W. *Methods Enzymol.* **1997**, *276*, 307.
30. Vagin, A.; Teplyakov, A. *J. Appl. Cryst.* **1997**, *30*, 1022.
31. McCoy, A. J.; Grosse-Kunstleve, R. W.; Adams, P. D.; Winn, M. D.; Storoni, L. C.; Read, R. J. *J. Appl. Cryst.* **2007**, *40*, 658.
32. Murshudov, G. N.; Vagin, A. A.; Dodson, E. J. *Acta Crystallogr., Sect. D* **1997**, *53*, 240.
33. McRee, D. E. *J. Struct. Biol.* **1999**, *125*, 156.